Avrupa Bilim ve Teknoloji Dergisi
Sayı 53, S. 112-125, Ocak 2024

Araştırma Makalesi

www.ejosat.com ISSN:2148-2683

European Journal of Science and Technology
No. 53, pp. 112-125, January 2024

Research Article

Guidance and Control of a Short-Range Air-to-Surface Missile Using an Angle-Based Switched Guidance Approach

Bülent Özkan[1], Harun Gökçe[2*]

[1] Gazi University, Faculty of Engineering, Mechanical Engineering Depart., Ankara, Turkey (ORCID: 0000-0003-3112-9723), bozkan@gazi.edu.tr
[2*] Gazi University, Faculty of Technology, Industrial Design Engineering Depart., Ankara, Turkey (ORCID: 0000-0002-2702-0111), harungokce@gazi.edu.tr

(İlk Geliş Tarihi 19 Temmuz 2023 ve Kabul Tarihi 30 Aralık 2023)

(**DOI:** 10.5281/zenodo.10646702)

REFERENCE/ATIF: Özkan, B., Gökçe, H. (2024). Guidance and Control of a Short-Range Air-to-Surface Missile Using an Angle-Based Switched Guidance Approach. *European Journal of Science and Technology*, (53), 112-125.

Abstract

The success of homing missiles is dependent on the selected guidance law. As per their structures, the guidance laws have different performance characteristics. Namely, the linear homing guidance law results in smaller terminal miss distance than the proportional navigation guidance law. However, its maximum lateral acceleration requirement is higher. In this study, a switching algorithm is proposed to take the advantages of a selected set of guidance laws by applying on a short-range missile used in air-to-surface operations. As per the results of the simulations carried on the computer, it is witnessed that the switching scheme yields satisfactory terminal miss distance values. Moreover, the maximum acceleration need is reduced for the missile especially when its autopilot operates at a constant bandwidth value.

Keywords: Switching guidance, guidance and control, angle-based guidance, control actuation system, air-to-surface missile, short range missile.

Karadan Karaya Bir Merminin Burun Eyletim Kiti Kullanılarak Güdüm ve Denetimi

Öz

Güdümlü füzelerin başarısı seçilen güdüm kanununa bağlıdır. Yönlendirme kanunları yapıları itibariyle farklı performans özelliklerine sahiptir. Doğrusal güdüm rehberliği yasası, orantılı seyrüsefer kılavuzluğu yasasından daha küçük terminal kaçırma mesafesiyle sonuçlanır. Bununla beraber maksimum yanal ivme gereksinimi daha yüksektir. Bu çalışmada, havadan karaya operasyonlarda kullanılan kısa menzilli bir füze için seçilmiş bir dizi güdüm kanununun avantajlarından yararlanacak bir anahtarlama algoritması önerilmektedir. Bilgisayarda yapılan simülasyon sonuçlarına göre anahtarlama şemasının tatmin edici terminal kaçırma mesafesi değerleri verdiği görülmüştür. Ayrıca füzenin otopilotunun sabit bant genişliği değerinde çalışması durumunda maksimum hızlanma ihtiyacı da azalmıştır.

Anahtar Kelimeler: Satıhtan satha mühimmatlar, güdümlü mermi, güdüm ve kontrol, burun eyletim kiti, itme kararsızlığı.

[*] Corresponding Author: harungokce@gazi.edu.tr

1. Introduction

Homing missiles have become very popular within the last years. This is because they have high capability on hitting intended target more precisely than their guided counterparts without damaging the surrounding of the target [1].

The success of the guided munition is dependent on their guidance and control algorithm. In this sense, the guidance scheme is more determinative for the achievement than the control method because the guidance scheme generates the command signals to the munition control system, or autopilot. For this reason, several guidance approaches are proposed for the guided munition. Regarding the homing missiles, the proportional navigation guidance (PNG), augmented proportional navigation guidance (APNG), velocity pursuit guidance (VPG), parabolic homing guidance (PHG), linear homing guidance (LHG), and body pursuit guidance (BPG) law are encountered in the literature among the popular guidance methods. Depending on the strategy of the guidance laws, they have different characteristics in performance criteria. Namely, the LHG law leads smaller terminal miss distance than PNG law, but its maximum lateral acceleration requirement is higher [1-4].

For the sake of taking the benefits of all possible guidance laws, they can be utilized in a selective scheme. In this concept, the most convenient guidance law can be selected and then applied on the missile at certain instants of the engagement scenario. The study which deals with a two stage PNG law for impact time control can be given as an example for this approach. In the mentioned work, the effective navigation ratio of the PNG law is switched from 1 to 2 at a certain instant of terminal guidance. In other words, the proposed guidance scheme begins with the VPG law and then passed to the PNG law. At the end of the computer simulations, it is shown that the approach makes the missile reach the specified destination at the desired impact time [5]. To control the impact angle of a physically constrained missile, a switched-gain guidance technique based on the PNG law is also given along with the relevant computer simulations [6]. In another study, a similar two-stage guidance law scheme is suggested to control the impact angle as well as the impact time. In this algorithm, a non-singular sliding mode control-based guidance law is utilized in the first stage and then switched to the PNG law when the missile gets closer to the target. This way, it becomes possible to satisfy the specified impact time and impact angle requirements [7]. Also, different dual-control guidance techniques are proposed to increase the hitting accuracy of the homing missiles [8, 9, 10, 11].

In this study, a switched guidance scheme is constructed by involving the PNG, APNG, VPG, PHG, LHG, and BPG laws. In the suggested scheme, the guidance laws are arranged such that they generate the guidance commands in the form of the flight path angles of the missile. During application, all those laws are compared at the beginning of each time segment and the most suitable one is selected for the forthcoming segment as per the considered performance index. The performance index is designated to minimize the terminal miss distance quantity as well as the maximum acceleration requirement for the considered missile. This procedure is repeated for all the time segments on the engagement duration. Since there exist no dramatical variations on the amount of the guidance commands due to switching, the missile autopilot maintains its stability over all the engagement scenarios. The relevant computer simulations are conducted regarding a missile aimed at utilizing in short range engagements for air-to-surface operations against stationary and manoeuvring ground target models. Also, the bandwidth of the missile autopilots is considered both in constant and varying modes. At the end of the simulations, it is observed that the suggested switching guidance scheme produces smaller terminal miss distance and maximum lateral acceleration requirement especially when the bandwidth of the missile autopilot becomes unchanged. The attained results vary depending on the weighting gain values used in the performance index.

2. Dynamic Modelling of the Missile

In the extent of the study, an aerodynamically controlled single-part missile having canard-type control surfaces is dealt with as schematized in Fig. 1 where δi indicates the deflection of the control fins of the missile.

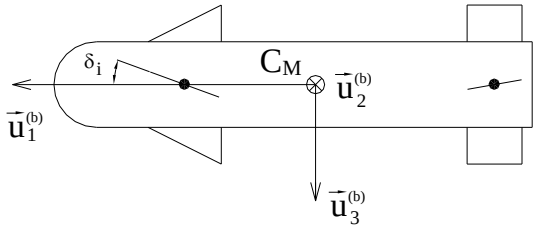

Figure 1. Single-part missile model [4] (Şekil 1. Tek parçalı füze modeli)

The governing differential equations of the missile describing its motion in space can be written as follows [4, 10]:

$$\dot{u} - rv + qw = (X + X_T)/m + g_x \quad (1)$$

$$\dot{v} + ru - pw = (Y + Y_T)/m + g_y \quad (2)$$

$$\dot{w} - qu + pv = (Z + Z_T)/m + g_z \quad (3)$$

$$\dot{p} = L/I_a \quad (4)$$

$$\dot{q} - pr = (M + M_T)/I_t \quad (5)$$

$$\dot{r} + pq = (N + N_T)/I_t \quad (6)$$

As C_M and $\vec{u}_i^{(b)}$ (i=*1, 2, and 3*) stand for the mass center of the missile and the unit vectors of the body-fixed reference frame F_b, respectively, the following definitions are made for the regarded missile configuration in Eqs. (1) through (6):

m: mass

I_a: axial moment of inertia component

I_t: transversal moment of inertia component

p, q and r: angular velocity components in the roll, pitch, and yaw directions

u, v and w: linear velocity components along $\vec{u}_1^{(b)}$, $\vec{u}_2^{(b)}$, and $\vec{u}_3^{(b)}$ directions

X, Y and Z: aerodynamic force components at point C_M along $\vec{u}_1^{(b)}$, $\vec{u}_2^{(b)}$, and $\vec{u}_3^{(b)}$ directions

L, M and N: aerodynamic moment components in the roll, pitch, and yaw directions

X_T, Y_T and Z_T: components of the thrust force vector at point C_M

L_T, M_T and N_T: thrust misalignment moment vector components

g_x, g_y and g_z: gravity vector components at point C_M

The present work deals with the terminal phase of the guidance scheme for the missile. Thus, the governing differential equations describing the motion of the missile in the space given Eqs. (1) through (6) are reduced to the forms below by regarding the end of thrust in this phase [4]:

$$\dot{u} - rv + qw = (X/m) + g_x \quad (7)$$

$$\dot{v} + ru - pw = (Y/m) + g_y \quad (8)$$

$$\dot{w} - qu + pv = (Z/m) + g_z \quad (9)$$

$$\dot{p} = L/I_a \quad (10)$$

$$\dot{q} - pr = M/I_t \quad (11)$$

$$\dot{r} + pq = N/I_t \quad (12)$$

The aerodynamic terms within Eqs. (7) through (12) are expressed as functions of the dynamic pressure (q_∞), missile cross-sectional area (S_M), and missile diameter (d_M) as follows [4, 10]:

$$X = C_x q_\infty S_M \quad (13)$$

$$Y = C_y q_\infty S_M \quad (14)$$

$$Z = C_z q_\infty S_M \quad (15)$$

$$L = C_l q_\infty S_M d_M \quad (16)$$

$$M = C_m q_\infty S_M d_M \quad (17)$$

$$N = C_n q_\infty S_M d_M \quad (18)$$

As ρ stands for the density of air at the designated altitude and $\pi \approx 3.14$, q_∞ and S_M can be obtained as [4]:

$$q_\infty = (1/2)\rho v_M^2 \quad (19)$$

$$S_M = (\pi/4)d_M^2 \quad (20)$$

Denoting the absolute value of the velocity vector of the missile by v_M, the aerodynamic coefficients C_x, C_y, C_z, C_l, C_m and C_n parameters are expanded into linear expressions in terms of the angle of attack (α), side-slip angle (β), aileron, elevator, and rudder deflections (δ_a, δ_e and δ_r) p, q and r as given below [4]:

$$C_x = C_{x0} \quad (21)$$

$$C_y = C_{y_\beta}\beta + C_{y_\delta}\delta_r + C_{y_r}\tau r \quad (22)$$

$$C_z = C_{z_\alpha}\alpha + C_{z_\delta}\delta_e + C_{z_q}\tau q \quad (23)$$

$$C_l = C_{l_\delta}\delta_a + C_{l_p}\tau p \quad (24)$$

$$C_m = C_{m_\alpha}\alpha + C_{m_\delta}\delta_e + C_{m_q}\tau q \quad (25)$$

$$C_n = C_{n_\beta}\beta + C_{n_\delta}\delta_r + C_{n_r}\tau r \quad (26)$$

Here, $\tau = d_M/(2v_M)$ and C_{x0} denotes a static aerodynamic axial force component. Moreover, the stability derivatives represented by C_{y_β}, C_{y_δ}, C_{y_r}, C_{z_α}, C_{z_δ}, C_{z_q}, C_{l_δ}, C_{l_p}, C_{m_α}, C_{m_δ}, C_{m_q}, C_{n_β}, C_{n_δ} and C_{n_r} are functions of Mach number (M_∞). During the simulations carried on the computer, the gains are updated continuously as per the present corresponds of the relevant flight parameters. In Eqs. (21) through (26), α and β are defined in the next manner [4]:

$$\alpha = arctan(w/u) \tag{27}$$

$$\beta = arcsin(v/v_M) \tag{28}$$

Beside these expressions δ_a, δ_e, δ_r are the angular deflections realized by the aerodynamic control surfaces and are described using the fin deflections as follows [4]:

$$\delta_a = (\delta_1 + \delta_3)/2 \tag{29}$$

$$\delta_e = (\delta_2 - \delta_4)/2 \tag{30}$$

$$\delta_r = (\delta_1 - \delta_3)/2 \tag{31}$$

3. Guidance Law

The proposed switched guidance approach is established by regarding the PNG, APNG, VPG, PHG, LHG, and BPG laws such that their commands are generated as to be reference signals in the sense of the missile flight path angle components.

3.1. Proportional Navigation Guidance Law

According to the PNG law, the command acceleration components of the missile, i.e. a_y^c and a_p^c, can be written in the yaw and pitch planes in the forthcoming way [4]:

$$a_y^c = N_y v_M\left[\dot{\lambda}_y\, cos(\gamma_m) - \dot{\lambda}_p\, sin(\gamma_m)\, sin\left(\lambda_y - \eta_m\right)\right] \tag{32}$$

$$a_p^c = -N_p v_M \dot{\lambda}_p\, cos\left(\lambda_y - \eta_m\right) \tag{33}$$

where Ny and Np stand for the effective navigation ratios in the yaw and pitch planes, λy and λp indicate the yaw and pitch components of the line-of-sight (LOS) angle, and ηm and γm denote the missile flight path angle components in the yaw and pitch planes.

Dividing the acceleration commands in Eqs. (32) and (33) by vM, they are converted to the commands for guidance in terms of the rates of the flight path angles, i.e. $\dot{\gamma}_m^c$ and $\dot{\eta}_m^c$:

$$\dot{\eta}_m^c = N_y\left[\dot{\lambda}_y\, cos(\gamma_m) - \dot{\lambda}_p\, sin(\gamma_m)\, sin\left(\lambda_y - \eta_m\right)\right] \tag{34}$$

$$\dot{\gamma}_m^c = -N_p \dot{\lambda}_p\, cos\left(\lambda_y - \eta_m\right) \tag{35}$$

As t_1 and t_2 indicate the initial and final time instants of each discrete integration segment, the integration of Eqs. (34) and (35) over time yields the PNG commands in flight path angles, i.e. η_m^c and γ_m^c as done below:

$$\eta_m^c = \int_{t_1}^{t_2} \dot{\eta}_m^c dt \tag{36}$$

$$\gamma_m^c = \int_{t_1}^{t_2} \dot{\gamma}_m^c dt \tag{37}$$

3.2. Augmented Proportional Navigation Guidance Law

Adding the half amount of the lateral component of the considered lateral acceleration of the target in the considered engagement plane to the PNG commands in Eqs. (32) and (33), then the acceleration commands can be determined as per the APNG law [4]. In a similar manner for the PNG law, the division of the mentioned acceleration commands by v_M results in the APNG commands in terms of $\dot{\eta}_m^c$ and $\dot{\gamma}_m^c$ in the next form:

$$\dot{\eta}_m^c = -N_y\left\{\dot{\lambda}_p\, cos\left(\lambda_y - \eta_m\right) + \left[a_T^t\, cos(\eta_m - \eta_t) + a_T^n\, sin(\eta_m - \eta_t)\right] sin(\gamma_m)\,/(2v_M)\right\} \tag{38}$$

$$\dot{\gamma}_m^c = N_p\left\{\dot{\lambda}_y\, cos(\gamma_m) - \dot{\lambda}_p\, sin(\gamma_m)\, sin\left(\lambda_y - \eta_m\right) + \left[a_T^n\, cos(\eta_m - \eta_t) - a_T^t\, sin(\eta_m - \eta_t)\right]/(2v_M)\right\} \tag{39}$$

where a_T^t and a_T^n represent the target acceleration vector components in the tangential and normal directions and η_t denotes the target heading angle on the horizontal plane. Eventually, the flight path angle commands of the APNG law, i.e. η_m^c and γ_m^c, can be generated by considering Eqs. (36) and (37).

3.3. Velocity Pursuit Guidance Law

The VPG guidance commands aiming at coinciding the missile velocity vector with the LOS vector can simply be determined by inserting unity to N_y and N_p to be unity in Eqs. (34) and (35) [4].

3.4. Parabolic Homing Guidance Law

Driving the missile towards an intended target point by forcing it to follow a parabolic trajectory, the PHG dictates the guidance commands in the acceleration form as follow [11]:

$$a_y^c = (d_1 + \mathrm{d}_2)\, sin(\gamma_m) + d_3\, cos(\gamma_m) \tag{40}$$

$$a_p^c = -d_1\, sin(\eta_m) + d_2\, cos(\eta_m) \tag{41}$$

As the symbols v_{Ti} and a_{Ti} refer to the target velocity components nd acceleration vectors on axis i=xyz respectively. Forthcoming definitions are made in Eqs. (40) and (41) where Δ_t stands for the duration for the missile to reach the prescribed intercept point from its current position and Δ_x, Δ_y, and Δ_z denotes the relative position vector components between missile and target:

$$d_1 = 2[(v_{Tx} - v_M\, cos(\eta_m)\, cos(\gamma_m))/\Delta t - (\Delta x/\Delta t^2)] + a_{Tx}$$

$$d_2 = 2\big[\big(v_{Ty} - v_M\, sin(\eta_m)\, cos(\gamma_m)\big)/\Delta t - (\Delta y/\Delta t^2)\big] + a_{Ty}$$

$$d_3 = 2[(v_{Tz} + v_M\, sin(\gamma_m))/\Delta t - (\Delta z/\Delta t^2)] + a_{Tz}$$

Applying the same approach as the cases with the PNG, APNG, and VPG laws, the flight path angle rate commands can be produced for the PHG law when the expressions in Eqs. (40) and (41) are divided by v_M:

$$\dot{\eta}_m^c = [(d_1 + \mathrm{d}_2)\, sin(\gamma_m) + d_3\, cos(\gamma_m)]/v_M \tag{42}$$

$$\dot{\gamma}_m^c = [-d_1\, sin(\eta_m) + d_2\, cos(\eta_m)]/v_M \tag{43}$$

The corresponding flight path angle commands come into the picture when Eqs. (42) and (43) are subjected to the time integration as given within Eqs. (36) and (37).

3.5. Linear Homing Guidance Law

Unlike the PHG law, the missile is intended to be oriented towards the target by dictating a linear trajectory so as to keep it always on the collision triangle, which is formed by the considered missile, intended target, and predicted intercept point. For this method, the flight path angles are directly generated as the resultant guidance commands in the following manner [4, 10, 11]:

$$\eta_m^c = arctan\big[\big(v_{Ty}\Delta t - \Delta y\big)/(v_{Tx}\Delta t - \Delta x)\big] \tag{44}$$

$$\gamma_m^c = arctan\left[\frac{\Delta z - v_{Tz}\Delta t}{(v_{Tx}\Delta t - \Delta x)\, cos(\eta_m) + (v_{Ty}\Delta t - \Delta y)\, sin(\eta_m)}\right] \tag{45}$$

3.6. Body Pursuit Guidance Law

Since it is necessary in the BPG law to align the missile longitudinal axis with the LOS vector, the commands for the guidance in the yaw and pitch planes (ψ_c and θ_c) can be derived as ψ and θ denote the yaw and pitch angles of the missile [4]:

$$\psi^c = \lambda_y \tag{46}$$

$$\theta^c = \lambda_p \tag{47}$$

Using the BPG commands in Eqs. (46) and (47), the corresponding flight path angle commands can be obtained using the next kinematic relationships [4]:

$$\eta_m^c = \psi^c + [\beta/\, cos(\theta)] \tag{48}$$

$$\gamma_m^c = \theta^c - \alpha \tag{49}$$

4. Switching Guidance Schema

In order to take the advantages of the mentioned guidance laws, a compound guidance scheme is proposed in the present study. In this extent, the guidance laws are arranged to yield their command signals in terms of the flight path angles of the missile and they are compared in accordance with a designated performance index momentarily. At each decision instant, the guidance law which makes the performance index minimum is selected.

As indicated in the related studies, the parameters of the terminal miss distance and maximum acceleration requirement have a significant role in choosing the most convenient guidance law. For the same engagement conditions, the total engagement time does not change considerably [4, 10, 11]. Regarding this fact, the performance index is designated by accounting the terminal miss distance in addition to the maximum acceleration requirement criteria in this study.

For a successful interception of missile and target, their velocity components normal to the LOS should be equal [12, 13]. Regarding the missile-target engagement geometry, this condition can be expressed in mathematical sense for the yaw and pitch planes as follows:

$$v_M\, sin\big(\eta_m - \lambda_y\big) = v_T\, sin\big(\eta_t - \lambda_y\big) \tag{50}$$

$$v_M \sin(\gamma_m - \lambda_p) = v_T \sin(\gamma_t - \lambda_p) \quad (51)$$

where v_T and γ_t stand for the target velocity vector magnitude and the heading angle of the target on the vertical plane, respectively. Hence, the flight path angle components required for a successful intercept i.e. η_{int} and γ_{int} are picked from Eqs. (50) and (51) as given below:

$$\eta y \sin\left[v_T \sin(\eta_t - \lambda_y)/v_M\right]_{int} \quad (52)$$

$$\gamma p \sin\left[v_T \sin(\gamma_t - \lambda_p)/v_M\right]_{int} \quad (53)$$

The error terms calculated as the difference between the ideal and reference flight path angle values in both planes (e_η and e_γ) can be introduced in the forthcoming fashion:

$$e_\eta = |\eta_{int} - \eta_m^c| \quad (54)$$

$$e_\gamma = |\gamma_{int} - \gamma_m^c| \quad (55)$$

The lower e_η and e_γ in Eqs. (54) and (55) results in the smaller the terminal miss distance.

As mentioned above, another criterion in deciding on the performance of the guidance laws is the maximum acceleration requirement of the missile. Since the final guidance stage called the terminal guidance phase with no thrust is handled in the present engagement scenarios, the tangential component of the missile is out of concern. Thus, only lateral component of the missile acceleration vector will be under consideration. Regarding that the absolute value of the instantaneous velocity vector of the missile does not change so much in all guidance laws, the squares of the flight path angles correspond to the lateral components of the linear acceleration. Once the sum of the squares of the rates of the flight path angles are kept as small as possible, the resulting total requirement on the acceleration components of the missile in lateral sense will become in a minimum level. Regarding the two criteria introduced above, the performance index (J) for switching is established as follows:

$$J = \int_{t_0}^{t_F} k_a\left(e_\eta^2 + e_\gamma^2\right) + k_r(\dot{\eta}_m^2 + \dot{\gamma}_m^2)\, dt \quad (56)$$

where k_a and k_r denote the weighting gains corresponding to the terminal value of the miss distance and maximum acceleration requirement, respectively. Also, t_0 and t_F stand for the initial and final time instants. In order to normalize the gains, they are selected such that they satisfy the condition of $\sqrt{k_a^2 + k_r^2} = 1$.

5. Angle Control System

For the conversion of the guidance commands yielded by the guidance laws to physical motion, an angle control system is designed by accounting the integral of the error defined between the reference and actual quantities belonging to the controlled state variable, i.e. flight path angle, is introduced as an additional state variable (x_i).

As the gravity is taken as external disturbance, it makes sense to designate the forthcoming state feedback control law in both the pitch plane separately to make the control of the corresponding fight path angle of the missiles [11]:

$$u = \delta_e = k_\gamma(\gamma_m^c - \gamma_m) - k_\theta\theta - k_q q + k_i x_i \quad (57)$$

where k_γ, k_θ, k_q, and k_i show the gains of the controller for the relevant state variables i.e. γ_m, θ, q, and x_i.

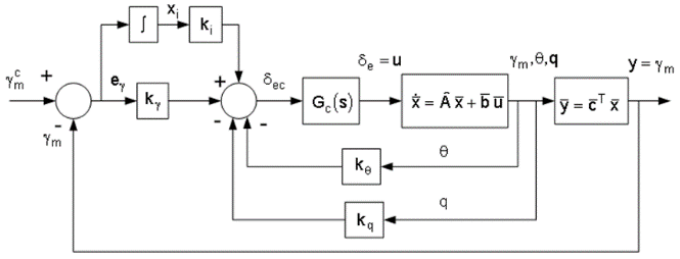

Figure 2. Angle control system [4] (Şekil 2. Açı kontrol sistemi)

Arranging the expressions denoting the missile motion, the closed loop transfer function i.e. γ_m^c and γ_m can be obtained between the amount of the desired and actual flight path angles in the pitch plane according to Fig. 2 as follows [4]:

$$\frac{\gamma_m(s)}{\gamma_m^c(s)} = \frac{n_{\gamma 3}s^3 + n_{\gamma 2}s^2 + n_{\gamma 1}s + 1}{d_{\gamma 4}s^4 + d_{\gamma 3}s^3 + d_{\gamma 2}s^2 + d_{\gamma 1}s + 1} \quad (58)$$

where, as the letter "s" indicates the variable of the Laplace transformation,

$n_{\gamma 1} = \left(k_\gamma a_{\alpha\delta} + k_i a_{\delta q}\right)/(k_i a_{\alpha\delta})$,

$n_{\gamma 2} = \left(a_{\alpha\delta} a_{\delta q} k_\gamma + a_{\alpha\delta} k_i Z_\delta\right)/(a_{\alpha\delta} a_{\alpha\delta} k_i)$,

$n_{\gamma 3} = \left(Z_\delta k_\gamma\right)/(a_{\alpha\delta} k_i)$,

$d_{\gamma 1} = \left[a_{\alpha\delta}\left(k_\theta + k_\gamma\right) + k_i a_{\delta q}\right]/(k_i a_{\alpha\delta})$,

$d_{\gamma 2} = \left(M_\alpha + M_\delta k_\theta - a_{\alpha q} + a_{\alpha\delta} k_q + a_{\delta q} k_\gamma + Z_\delta k_i\right) / (k_i a_{\alpha\delta})$,

$d_{\gamma 3} = \left[M_\delta k_q + Z_\delta k_\gamma - \left(M_q + Z_\alpha\right)\right]/(k_i a_{\alpha\delta})$,

$d_{\gamma 4} = 1/(k_i a_{\alpha\delta})$; $a_{\alpha\delta} = M_\delta Z_\alpha - M_\alpha Z_\delta$,

$a_{\delta q} = M_\delta Z_q - M_q Z_\delta$, and $a_{\alpha q} = M_q Z_\alpha - M_\alpha Z_q$.

The characteristic polynomial of the transfer function in Eqn. (58) is given below:

$$D(s) = d_{\gamma 4} s^4 + d_{\gamma 3} s^3 + d_{\gamma 2} s^2 + d_{\gamma 1} s + 1 \tag{59}$$

In order to obtain the gains of the controller i.e. k_γ, k_θ, k_q and k_i the fourth-order Butterworth polynomial described in Eq. (60) can be utilized in the pole placement again with a damping ratio of 0.707 [4]:

$$B_4(s) = (1/\omega_c^4)s^4 + (2.613/\omega_c^3)s^3 + (3.414/\omega_c^2)s^2 + (2.613/\omega_c)s + 1 \tag{60}$$

where ω_c denotes the assigned bandwidth value in *rad/s*. Comparing Eq. (59) to Eq. (60), the matrix equation to solve k_γ, k_θ, k_q and k_i becomes:

$$[k_\gamma \quad k_\theta \quad k_q \quad k_i]^T = \widehat{M}_k^{-1} \bar{b}_k \tag{61}$$

where $\widehat{M}_k = \begin{bmatrix} 0 & 0 & 0 & a_{\alpha\delta} \\ Z_\delta & 0 & M_\delta & \frac{-2.613 a_{\alpha\delta}}{\omega_c^3} \\ a_{\delta q} & M_\delta & a_{\alpha\delta} & Z_\delta - \frac{3.414 a_{\alpha\delta}}{\omega_c^2} \\ a_{\alpha\delta} & a_{\alpha\delta} & 0 & a_{\alpha q} - \frac{2.613 a_{\alpha\delta}}{\omega_c} \end{bmatrix}$, and $\bar{b}_k = \begin{bmatrix} \omega_c^4 \\ M_q + Z_\alpha \\ a_{\alpha q} - M_\alpha \\ 0 \end{bmatrix}$.

Similar to the pitch plane derivation, the transfer function of the closed-loop transfer function belonging to the flight path angle control system can be adapted to the yaw plane from the control system in the pitch plane using the same structure by introducing $n_{\eta 1}$, $n_{\eta 2}$, $n_{\eta 3}$, $d_{\eta 1}$, $d_{\eta 2}$, $d_{\eta 3}$, and $d_{\eta 4}$ [4]:

$$\frac{\eta_m(s)}{\eta_m^c(s)} = \frac{n_{\eta 3} s^3 + n_{\eta 2} s^2 + n_{\eta 1} s + 1}{d_{\eta 4} s^4 + d_{\eta 3} s^3 + d_{\eta 2} s^2 + d_{\eta 1} s + 1} \tag{62}$$

Similar to the pitch plane derivation, the transfer function of the closed-loop transfer function belonging to the flight path angle control system can be adapted to the yaw plane from the control system in the pitch plane using the same structure by introducing $n_{\eta 1}$, $n_{\eta 2}$, $n_{\eta 3}$, $d_{\eta 1}$, $d_{\eta 2}$, $d_{\eta 3}$, and $d_{\eta 4}$ [4].

In this study, the angle autopilots are operated in two different modes in one of which the bandwidth [fc(t)] is maintained constant throughout the whole computer simulations. In the second mode, the initial value of the bandwidth reaches its designated final value at the end of a specified time duration and then it remains at that level till the termination of the related simulation for the sake of diminishing the high initial requirement for the acceleration of the relevant guidance law as formulated below [4]:

$$f_c(t) = \begin{cases} a \cdot t + b & , \quad for t_0 \le t < t_F \\ f_c(t_F) & , \quad for t \ge t_F \end{cases} \tag{63}$$

where $a = [f_c(t_0) - f_c(t_F)]/(t_0 - t_F)$, and $b = [f_c(t_F) t_0 - f_c(t_0)] t_F/(t_0 - t_F)$.

6. Target Kinematics

Assuming that the change in altitude is negligible, the motion of the ground target is described on the horizontal plane. In this consideration, the normal and tangential acceleration components of the target, (a_T^n and a_T^t) v_T and η_t are taken into account. Introducing a_T^n and a_T^t in addition to the initial target velocity values and heading angle (v_{T0} and η_{t0}) v_T and η_t are calculated depending on time i.e. t, by the next integral functions with σ denoting the integration variable [4]:

$$v_T(t) = v_{T0} + \int_{t_0}^{t} a_T^t(\sigma) d\sigma \tag{64}$$

$$\eta_t(t) = \eta_{t0} + \int_{t_0}^{t} [a_T^n(\sigma)/v_T(\sigma)] d\sigma \tag{65}$$

Regarding their initial values (x_{T0}, y_{T0} and z_{T0}) the target position can be described by the next expressions on the horizontal plane as functions of time:

$$x_T(t) = x_{T0} + \int_{t_0}^{t} v_T(\sigma) \cos\left(\eta_t(\sigma)\right) d\sigma \tag{66}$$

$$y_T(t) = y_{T0} + \int_{t_0}^{t} v_T(\sigma)\, sin\big(\eta_t(\sigma)\big)\, d\sigma \quad (67)$$

$$z_T(t) = z_{T0} \quad (68)$$

Here, since z_{T0} is much smaller than x_{T0} and y_{T0}, it is treated to be constant throughout the engagement.

7. Missile-Target Engagement Model

Ther engagement geometry between the missile and target can be described by the following relationships where $r_{T/M}$ stands for the magnitude of the LOS vector ($\vec{r}_{T/M}$) [4]:

$$r_{T/M} = \sqrt{\Delta x^2 + \Delta y^2 + \Delta z^2} \quad (69)$$

$$\lambda_p = arctan\big[-\Delta z\, cos\big(\lambda_y\big)/\Delta x\big] \quad (70)$$

$$\lambda_y = arctan(\Delta y/\Delta x) \quad (71)$$

$$d_{miss} = \sqrt{\Delta x^2(t_F) + \Delta y^2(t_F)} \quad (72),$$

The calculation of the total miss distance at the end of the engagement (d_{miss}) at $t=t_F$ where t_F represents the final time of the engagement is made using the next expression by regarding the condition in which the vertical component of $r_{T/M}$ vanishes i.e. $\Delta_z=0$ [4].

8. Computer Simulation

Regarding the PNG, APNG, VPG, PHG, LHG, and BPG laws whose commands are in the flight path angles, computer simulations are performed for the terminal guidance phase of the missile by considering stationary and maneuvering targets. In the simulations, the considered guidance laws are first applied to the missile from the beginning to the termination of the engagement scenarios. Then, they are utilized in a switching algorithm explained above. In the switching scheme, three different cases are taken into consideration for 1, 0.5, and 0 values of k_a. The maneuvering target has the lateral acceleration of 0.3·g (g=9.81 m/s^2) and initial speed of 80 km/h. The effective navigation ratios of the PNG and APNG laws (N_y and N_p) are selected to be 3 and bandwidth of both control systems taking the control variables as acceleration and angular displacement are set to 5 Hz (ω_c= 31.4 rad/s) [4]. The engagement simulations are ceased while the vertical component of the relative position vector becomes below 0.5 m between the missile and target.

Moreover, the control actuation system in the missile control system is modeled in the form of a second-order system possessing a 20 Hz bandwidth value. Also, the operating frequencies are set to 110 Hz for the gyroscopes and accelerometers [4, 8]. In the computer simulations, the numerical values are considered for the essential as given in Table 1. The mentioned numerical values of the missiles are selected in a manner compatible with the dimensions and inertial parameters of a tactical 2.75 inches air-to-surface missile.

Table 1. Essential parameters for the single-part missile [4] (Tablo 1. Tek parçalı füze için temel parametreler)

Parameter	Symbol	Value
Diameter	d_M	*70 mm*
Cross-Sectional Area	S_M	*3848.5 mm^2*
Total Length	L_M	*2000 mm*
Total Mass	m	*17.55 kg*
Axial Moment of Inertia	I_a	*0.0214 kg·m^2*
Transversal Moment of Inertia	I_t	*5.855 kg·m^2*
Acceleration Limit of the Missile	a_{max}	*30·g (g=9.81 m/s^2)*

The aerodynamic coefficients in the model are calculated by regarding the M_∞ range of 0.5 to 1.5, δ_a, δ_e and δ_r ranges of -20 to 20°, and α and β ranges of -9 to 9° using the Missile Datcom software. During the simulations the aerodynamic coefficients are continuously updated using relevant look-up tables prepared for the ranges given above. The initial values are submitted in Table 2 for the missile and target kinematic parameters in the conducted engagement scenarios are.

The related simulations are performed using the MATLAB© Simulink© software for the constant and varying bandwidth cases of the angle autopilots taking the comparison criteria to be the miss distance at the termination of the engagement, engagement time, and maximum acceleration demand. The data acquired from these simulations are submitted in Table 3 and Table 4 respectively.

The engagement geometry of the scenarios numbered 1, 10, 14, and 17 are submitted Fig. 3 through Fig. 6. For the scenarios in which the switching scheme is utilized, which guidance laws are chosen among the six laws in time as per the performance index in Eq. (56) are sampled with scenarios numbered 16, 17, 18, and 35 in Fig. 7 through Fig. 10. In these plots, the dicrete numbers are assigned to the guidance laws in the following manner: 1: LHG, 2: VPG, 3: PNG, 4: APNG, 5: PHG, and 6: BPG.

Table 2. Conditions for the missile-target engagement for the computer simulations (Tablo 2. Bilgisayar simülasyonları için füze-hedef angajmanı koşulları)

Parameter	Value	Parameter	Value	Parameter	Value
x_{M0}	0	q_0 and r_0	5 rpm	η_{t0}	0
y_{M0}	0	α_0 and β_0	0	a_T^t	0
z_{M0}	250 m	x_{T0}	5000 m	t_0	0
v_{M0}	510 m/s (M_∞=1.5)	y_{T0}	500 m	t_F	1 s
η_{m0} γ_{m0}	0	z_{T0}	0	$f_c(t_0)$	1 Hz
p_0	50 rpm	v_{T0}	22 m/s	$f_c(t_F)$	5 Hz

Table 3. Results of the computer simulations with constant bandwidth angle autopilots (Tablo 3. Sabit bant genişliği açılı otopilotlarla yapılan bilgisayar simülasyonlarının sonuçları)

Scenario Number	Target Type	Guidance Law	Terminal Miss Distance (m)	Total Engagement Time (s)	Maximum Acceleration Req. (g)
1	Stationary	PNG	9.643	16.687	14.252
2		APNG	10.030	16.686	14.252
3		VPG	9.037	16.690	14.252
4		PHG	9.905	16.690	14.252
5		LHG	8.938	16.690	14.252
6		BPG	504.429	12.711	355.711
7		Switching-k_a=1	6.121	16.793	14.260
8		Switching-k_a=0.5	6.652	16.774	14.252
9		Switching-k_a=0	6.769	16.759	14.252
10	Maneuvering	PNG	9.505	17.454	14.252
11		APNG	8.243	17.440	14.252
12		VPG	9.280	17.533	166.887
13		PHG	7.669	17.446	14.252
14		LHG	8.031	17.440	32.308
15		BPG	579.900	12.541	356.352
16		Switching-k_a=1	8.031	17.440	32.308
17		Switching-k_a=0.5	7.873	17.544	35.010
18		Switching-k_a=0	3.492	17.992	39.010

Table 4. Results of the computer simulations in the yaw plane with varying bandwidth angle autopilots (Tablo 4. Değişken bant genişliği açısına sahip otopilotlarla sapma düzlemindeki bilgisayar simülasyonlarının sonuçları)

Scenario Number	Target Type	Guidance Law	Terminal Miss Distance (m)	Total Engagement Time (s)	Maximum Acceleration Req.(g)
19	Stationary	PNG	8.271	16.703	6.490
20		APNG	9.867	16.670	6.490
21		VPG	8.332	16.701	6.352
22		PHG	8.036	16.704	6.423
23		LHG	7.293	16.708	6.353
24		BPG	506.418	12.197	387.218
25		Switching-k_a=1	9.330	16.797	6.036
26		Switching-k_a=0.5	9.342	16.796	6.034
27		Switching-k_a=0	8.076	16.802	6.035
28	Maneuvering	PNG	8.043	17.486	6.458
29		APNG	8.780	17.449	7.178
30		VPG	9.100	17.544	230.627
31		PHG	8.451	17.455	6.900
32		LHG	7.579	17.473	8.270
33		BPG	583.467	12.525	386.983
34		Switching-k_a=1	7.579	17.473	8.270
35		Switching-k_a=0.5	8.512	17.560	34.855
36		Switching-k_a=0	12.309	18.138	40.500

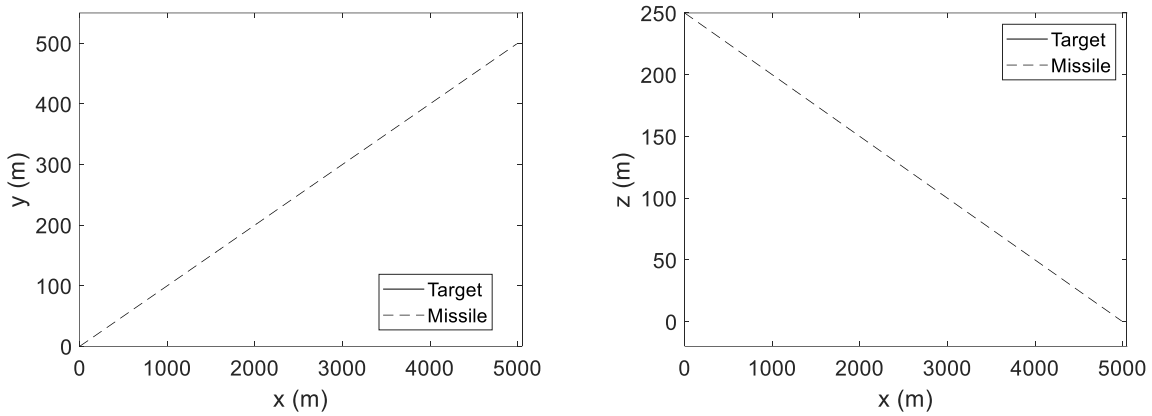

Figure 3. Engagement graph in scenario number 1 (Şekil 3. 1 numaralı senaryoda etkileşim grafiği)

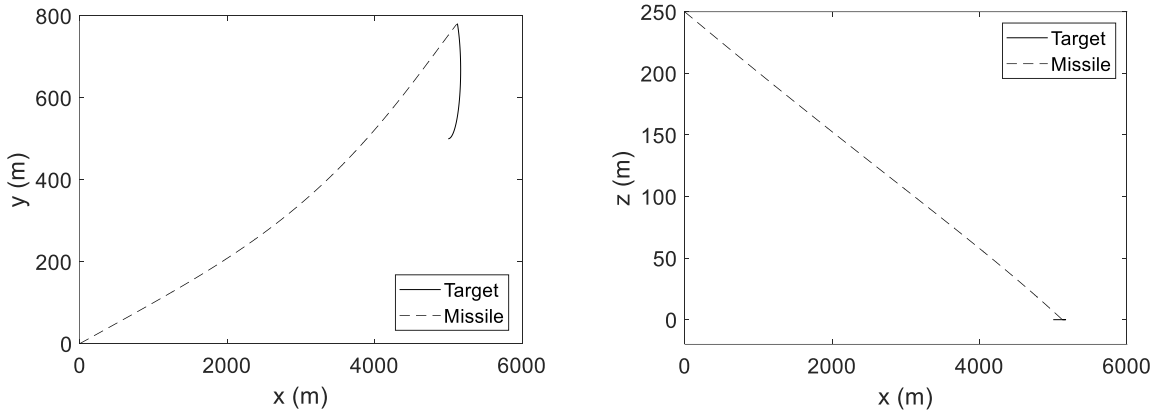

Engagement in Horizontal Plane Engagement in Vertical Plane

Figure 4. Engagement graph in scenario number 10 (Şekil 4. 10 numaralı senaryoda etkileşim grafiği)

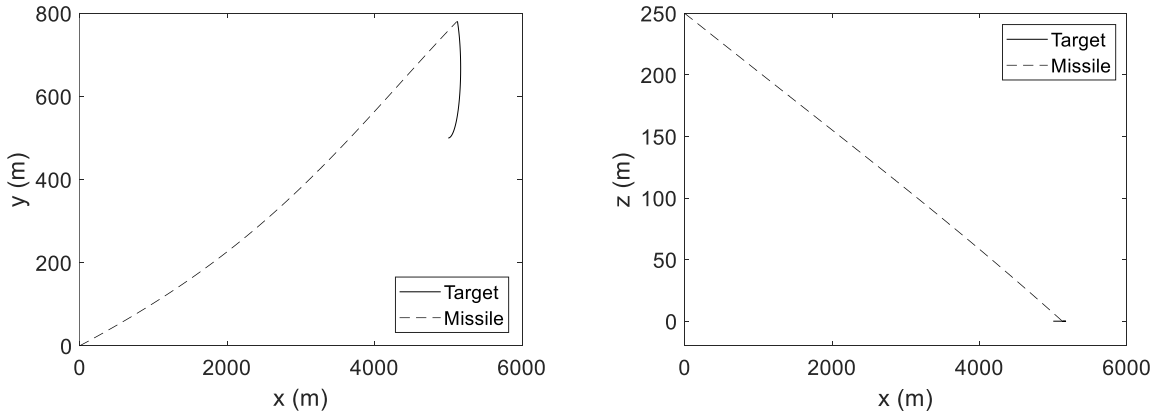

Engagement in Horizontal Plane Engagement in Vertical Plane

Figure 5. Engagement graph in scenario number 14 (Şekil 5. 14 numaralı senaryoda etkileşim grafiği)

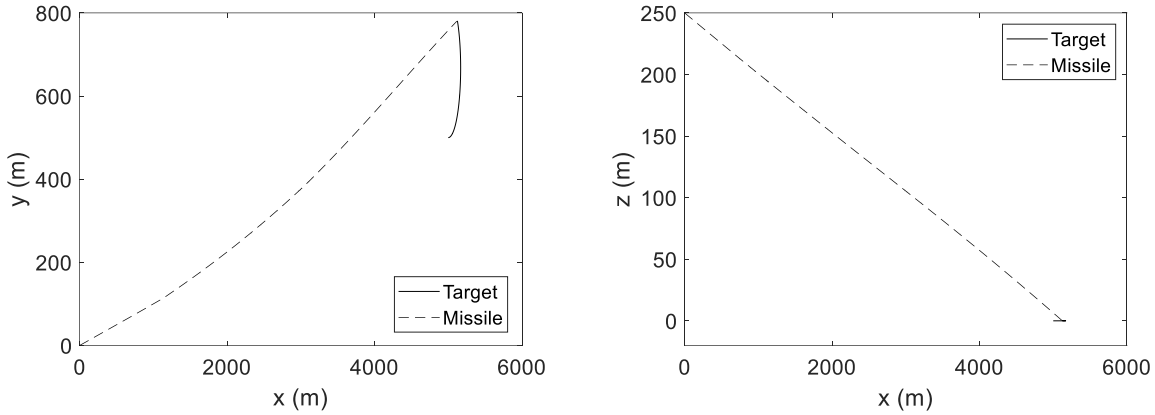

Engagement in Horizontal Plane Engagement in Vertical Plane

Figure 6. Engagement graph in scenario number 17 (Şekil 6. 17 numaralı senaryoda etkileşim grafiği)

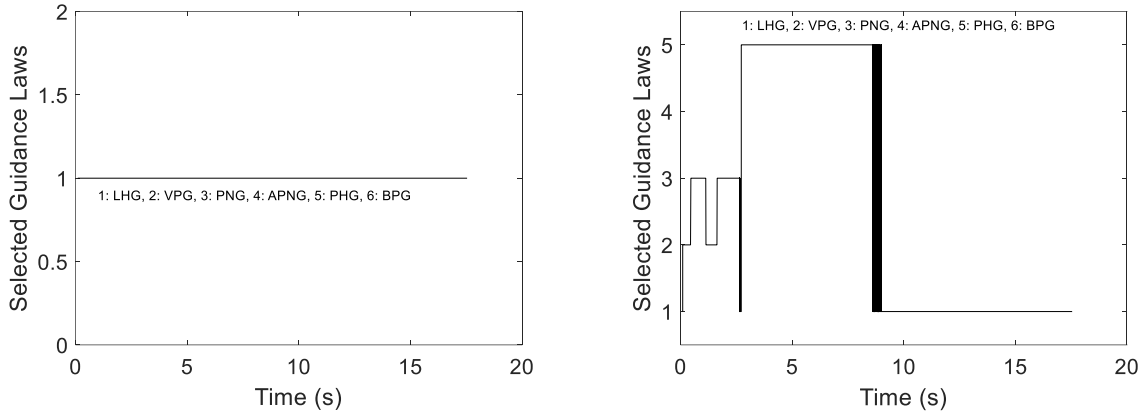

Figure 7. Selected guidance laws in scenario number 16 and number 17 (Şekil 7. 16 ve 17 numaralı senaryolarda seçilen yönlendirme yasaları)

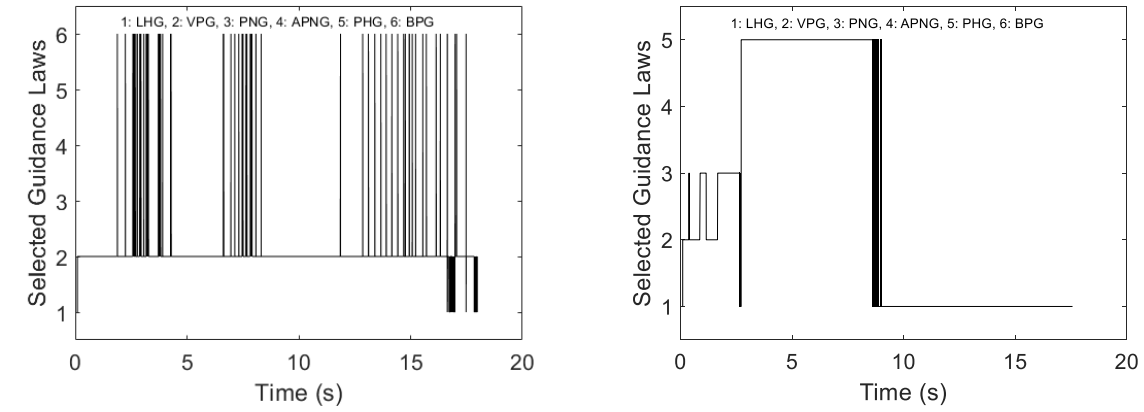

Figure 8. Selected guidance laws in scenario number 18 and number 35 (Şekil 8. 18 ve 35 numaralı senaryolarda seçilen yönlendirme yasaları)

8. Conclusions

Evaluating the data acquired from the computer simulations, it is seen that the proposed switching guidance algorithm yields small miss distance values compared to the other guidance laws depending on the engagement conditions and weighting gains. Here, the switching algorithm seems more successful when the missile autopilot operates at constant bandwidth values.

Although it produces smallest values with the autopilots having varying-bandwidth values against stationary targets, the algorithm does not provide an explicit advantage in the maximum acceleration requirements. Also, except the unsuccessful situations with the BPG law, the engagement time values happen to be almost the same regarding all the guidance laws under consideration. Even though the relevant simulation results are not presented in this study, it is observed that there exists almost no difference among the miss distance at the termination, engagement time, and maximum acceleration requirement values attained with these guidance laws including the switching guidance law when the resultant initial distance between the missile and target is below 3500 m.

As another consequence of this study, it is shown that guidance laws based on acceleration involving the PNG, APNG, VPG, and PHG laws can be turned into angle-based guidance laws leading satisfactory engagement results. Another interesting result of this work is that the BPG law which aims at coinciding the missile longitudinal axis with the LOS vector misses the target at a very large distance in all conditions considered.

Eventually, it can be concluded that the proposed switching guidance scheme can be applied to the missiles with an appropriate selection of weighting gains. As shown, better results should be expected if the related missile autopilot runs at a constant bandwidth value.

Nomenclature

a_{max} acceleration limit of the missile (m/s^2)
a_p^c component of the command acceleration to the missile in the pitch plane (m/s^2)
a_T^n component of the target acceleration vector in normal direction (m/s^2)
a_T^t component of the target acceleration vector in tangential direction (m/s^2)
a_{Tx} component of the target acceleration vector in longitudinal direction (m/s^2)
a_{Ty} component of the target acceleration vector in lateral direction (m/s^2)
a_{Tz} component of the target acceleration vector in vertical direction (m/s^2)
a_y^c component of the command acceleration to the missile in the yaw plane (m/s^2)
C_i aerodynamic force and moment components (i=x, y, z, l, m, n)
C_M mass center of the missile
$D(s)$ characteristic polynomial
d_M missile diameter (m)
d_{miss} miss distance at the termination of the engagement between the missile and target (m)
e_η error term for the flight path angle of the missile between its ideal and reference values of in the yaw plane (rad)
e_γ error term for the flight path angle of the missile between its ideal and reference values of in the pitch plane (rad)
F_b body-fixed reference frame of the missile
$f_c(t)$ bandwidth of the missile autopilot (Hz)
$f_c(t_0)$ bandwidth of the missile autopilot at the initial time instant
$f_c(t_F)$ bandwidth of the missile autopilot at the final time instant
g gravity (=9.81 m/s^2)
g_x gravity component acting on the missile mass center in longitudinal direction (m/s^2)
g_y gravity component acting on the missile mass center in lateral direction (m/s^2)
g_z gravity component acting on the missile mass center in vertical direction (m/s^2)
I_a moment of inertia component of the missile in axial sense (kg·m^2)
I_t moment of inertia component of the missile in a sense (kg·m^2)
J performance index for switching
k_a weighting gain corresponding to the terminal miss distance.
k_n pitch plane controller gains of the angle control system (n=γ, θ, q, and i)
k_r weighting gain corresponding to the maximum acceleration.
L roll component of the aerodynamic moment vector (N·m)
L_T thrust misalignment moment component in the roll direction.
M pitch component of the aerodynamic moment vector (N·m)
m mass of the missile (kg)
M_∞ Mach number
M_T thrust misalignment moment component in the pitch direction
N yaw component of the aerodynamic moment vector (Nm)
N_p effective navigation ratio in the pitch plane
N_T thrust misalignment moment component in the yaw direction (Nm)
N_y effective navigation ratio in the yaw plane
p roll velocity component of the missile (rad/s)
p_0 initial value of the roll angular velocity component of the missile (rad/s)
q pitch angular velocity component of the missile (rad/s)
q_0 initial value of the pitch angular velocity component of the missile (rad/s)
q_∞ dynamic pressure acting on the missile (Pa)
r yaw angular velocity component of the missile (rad/s)
r_0 initial value of the yaw angular velocity component of the missile (rad/s)
$\vec{r}_{T/M}$ line-of-sight vector (m)
$r_{T/M}$ absolute value of the line-of-sight vector (m)
s variable of the Laplace transformation
S_M cross-sectional area of the missile (m^2)

t time variable (s)
t_1 initial time instant of each discrete integration segment (s)
t_2 final time instant of each discrete integration segment (s)
t_0 initial time instant (s)
t_F final time instant (s)
u component of the missile velocity vector in longitudinal direction in the body-fixed reference frame (m/s)
$\rho_i^{(j)}$ unit vector of F_j in its i^{th} direction ($i=1$, 2 and 3)
v component of the missile velocity vector in lateral direction in the body-fixed reference frame (m/s)
v_M absolute value of the missile velocity vector (m/s)
v_T absolute value of the target velocity vector (m/s)
v_{T0} initial target velocity (m/s)
v_{Tx} component of the target velocity vector in longitudinal direction (m/s)
v_{Ty} component of the target velocity vector in lateral direction (m/s)
v_{Tz} component of the target velocity vector in vertical direction (m/s)
X component of the aerodynamic force vector in longitudinal direction (N)
x_i additional state variable in the angle control system
x_M component of the position vector of the missile mass center in longitudinal direction (m)
x_{M0} component of the initial position vector of the missile mass center in longitudinal direction (m)
X_T component of the thrust force vector at the mass center of the missile in longitudinal direction (N)
x_T component of the position vector of the target mass center in longitudinal direction (m)
x_{T0} component of the initial position vector of the target mass center in longitudinal direction (m)
w component of the missile velocity vector in vertical direction in the body-fixed reference frame (m/s)
Y component of the aerodynamic force vector in lateral direction
y_M component of the position vector of the missile mass center in lateral direction (m)
y_{M0} component of the initial position vector of the missile mass center in lateral direction (m)
Y_T component of the thrust force vector at the mass center of the missile in lateral direction (N)
y_T component of the position vector of the target mass center in lateral direction (m)
y_{T0} component of the initial position vector of the target mass center in lateral direction (m)
Z component of the aerodynamic force vector in vertical direction (N)
z_M component of the position vector of the missile mass center in vertical direction (m)
z_{M0} component of the initial position vector of the missile mass center in vertical direction (m)
Z_T component of the thrust force vector at the mass center of the missile in vertical direction (N)
z_T component of the position vector of the target mass center in vertical direction (m)
z_{T0} component of the initial position vector of the target mass center in vertical direction (m)
α angle of attack (rad)
α_0 initial value of the angle of attack (rad)
β side-slip angle (rad)
β_0 initial value of the side-slip angle (rad)
Δt duration from the initial time to the final time of the missile-target engagement (s)
Δx longitudinal component of the relative distance between the missile and target (m)
Δy lateral component of the relative distance between the missile and target (m)
Δz vertical component of the relative distance between the missile and target (m)
δ_a aileron deflection of the missile (rad)
δ_e elevator deflection of the missile (rad)
δ_I deflection of the i^{th} control fin ($i=1$, 2, 3, and 4) (rad)
δ_r rudder deflection of the missile (rad)
η_{int} flight path angle of the missile in the yaw plane for a successful intercept (rad)
η_m flight path angle of the missile in the yaw plane (rad)
η_{m0} initial value of the yaw plane flight path angle of the missile (rad)
η_m^c guidance command to the flight path angle of the missile in the yaw plane (rad)
η_t heading angle of the target on the horizontal plane (rad)
η_{t0} initial value of the heading angle of the target on the horizontal plane (rad)
γ_{int} flight path angle of the pitch plane missile in the for a successful intercept (rad)
γ_m flight path angle of the missile in the pitch plane (rad)
γ_{m0} initial value of the pitch plane flight path angle of the missile (rad)
γ_m^c guidance command to the flight path angle of the missile in the pitch plane (rad)
γ_t heading angle of the target on the vertical plane (rad)
λ_p pitch component of the line-of-sight angle (rad)
λ_y yaw component of the line-of-sight angle (rad)
ω_c desired bandwidth value (rad/s)

π "pi" number (=3.14)
ψ yaw angle of the missile (rad)
ψ_c guidance command to the yaw angle of the missile (rad)
ρ air density (kg/m^3)
θ pitch angle of the missile (rad)
θ_c guidance command to the pitch angle of the missile (rad)

Subscripts

0 initial
a i) axial ii) aileron
c i) command ii) control
e elevator
F final
M, m missile
p pitch
r i) roll ii) rudder
T i) target ii) thrust
t i) target ii) transversal
x longitudinal axis
y i) yaw ii) lateral axis
z vertical axis

References

1. Zarchan, P., Tactical and Strategic Missile Guidance, Vol. 157, Progress in Aeronautics and Astronautics, AIAA, Washington DC, 1994.
2. Zarchan, P., "Ballistic Missile Defense Guidance and Control Issues", Science and Global Security, Vol. 8, 1998, pp. 99-124.
3. Yang, C. D., Hsiao, F. B., and Yeh, F. B., "Generalized Guidance Law for Homing Missiles", IEEE Transactions on Aerospace and Electronic Systems, Vol. AES-25, No. 2, March 1989, pp. 197-212.
4. Özkan, B., Özgören, M. K., and Mahmutyazıcıoğlu, G., "Performance Comparison of the Notable Acceleration- and Angle-Based Guidance Laws for a Short-Range Air-to-Surface Missile", Turkish Journal of Electrical Engineering and Computer Sciences, Vol. 25, 2017, pp. 3591-3606. doi: 10.3906/elk-1601-230
5. Saleem, A. and Ratnoo, A., "Two Stage Proportional Navigation Guidance Law for Inpact Time Control", 2018 Indian Control Conference (ICC), IIT Kanpur, India, 2018.
6. Tekin, R. and Erer, K. S., "Switched-Gain Guidance for Impact Angle Control under Physical Constraints", Journal of Guidance, Control, and Dynamics, Vol. 38, No. 2, 2015, pp. 205-216. doi: 10.2514/1.G000766
7. Chen, X. And Wang, J., "Two-Stage Guidance Law with Impact Time and Angle Constraints", Nonlinear Dynamics, Vol. 95, 2019, pp. 2575-2590. doi: 10.1007/s11071-018-4710-3
8. Lee, H. I., Tahk, M. J., and Sun, B. C., "Practical Dual-Control Guidance Using Adaptive Intermittent Maneuver Strategy", Journal of Guidance, Control, and Dynamics, Vol. 24, No. 5, 2001, pp. 1009-1015.
9. Wang, Y., Shi, X., and Zhu, Y., "A Novel Switching Guidance Law against Hypersonic Random Maneuvering Target", 2010 Chinese Control and Decision Conference, China, 2010.
10. Özkan, B., Özgören, M. K., and Mahmutyazıcıoğlu, G., "Modeling of Dynamics, Guidance, and Control Systems of Air-to-Surface Missiles ", The Journal of Defense Modeling and Simulation: Applications, Methodology, Technology, Vol. 9, No. 2, 2012, pp. 101-112. doi: 10.1177/1548512911407647
11. Özkan, B., Özgören, M. K., and Mahmutyazıcıoğlu, G., "Comparison of the Linear Homing, Parabolic Homing and Proportional Navigation Guidance Methods on a Two-Part Homing Missile against a Surface Target", Gazi University Journal of Science, Vol. 23, No. 1, 2010, pp. 81-87.
12. Çilek, B., Missile Guidance with Impact Angle Constraint, Ms.C. Thesis, Aerospace Engineering Department, Middle East Technical University, Turkey, 2014.
13. Zhang, H., Tang, S., Guo, J., and Zhang, W., "A Two-Phased Guidance Law for Impact Angle Control with Seeker's Field-of-View Limit", Hindawi International Journal of Aerospace Engineering, Vol. 2018, 2018, pp. 1-13. doi: 10.1155/2018/7403639